

Universal, transferable and targeted adversarial attacks

Junde Wu

Harbin Institute of Technology

wujunde@hit.edu.cn

Rao Fu

Harbin Institute of Technology

Abstract

Deep Neural Network has been found vulnerable recently. A kind of well-designed inputs, which called adversarial examples, can lead the networks to make incorrect predictions. Depending on the different scenarios, goals and capabilities, the difficulty to generate the attack is different. For example, generating a targeted attack is more difficult than a non-targeted attack, a universal attack is more difficult than a non-universal attack, a transferable attack is more difficult than a nontransferable one. The question is: Is there exist an attack that can survival in the most harsh adversity to meet all these requirements. Although many cheap and effective attacks have been proposed, this question is still not completely solved over large models and large scale dataset. In this paper, we learn a universal mapping from the sources to the adversarial examples. These examples can fool classification networks into classifying all of them to one targeted class. Besides, they are also transferable between different models. Our code is released at:

1. Introduction

Deep Neural Network has outperformed many previous techniques in a wide domain. Their high accuracy and fast speed make them to be widely deployed in applications. Despite these great successes, it has been found vulnerable to the adversarial examples: the output of the networks can be manipulated by adding a kind of meticulously crafted subtle perturbations to the input data. This property is shown to be generally exist. Whether in the tasks of computer vision, like classification [24], objection detection [26], semantic segmentation [4] or in tasks of Natural Language Processing [9] and Reinforcement Learning [7].

In the classification task, the adversarial attacks aim to manipulate the network to misclassify. Previous works have proved generating this kind of adversarial examples can be very cheap and effective [6]. But the difficulty of the attack varies with the adversarial goals, perturbation scope and adversary knowledge. To put it clearly, we taxonomize

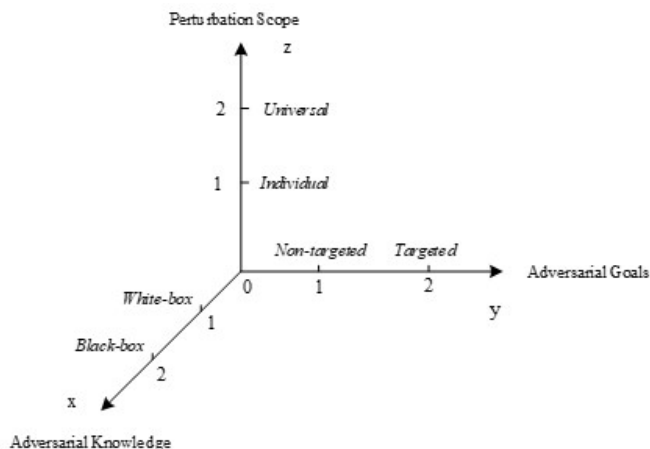


Figure 1: The taxonomy of adversarial attacks

the threat models by different goals, adversarys knowledge and perturbation scope. The taxonomy is shown in Figure 1.

- Adversarial Goals

- *Non-targeted misclassification* forces the victim model to incorrectly classify the input into an arbitrary class.

- *Targeted misclassification* forces the victim model to incorrectly classify all the inputs to a specific targeted class.

- Adversarial Knowledge

- *White-box attacks* assume threat model knows everything about the victim model, including the network architecture and the training dataset.

- *Black-box attacks* assume threat model can't get access to the victim model. It only knows the standard output of the network, like the labels of the inputs and the corresponding scores. But if the adversarial examples are transferable, a white-box attack can be transferred to a black-box model.

- Perturbation Scope

- *Individual attacks* solve the optimization problem for each single input. The perturbations for each clean input are all different.

- *Universal attacks* denote the attacks that are able to learn a universal mapping relation between the inputs and

adversarial examples, but don't need to solve the optimization problem for each input.

In Figure 1, the difficulty of the attacks increases with axes x, y, z . In this paper, we mainly explore how to produce attacks under the strictest conditions, which is correspond to point (2,2,2) in Figure 1, denoting the transferable, universal and targeted attacks.

In the following, we first discuss related work in section 2. We then propose low frequency fooling image in section 3. We introduce our method of producing adversarial examples in section 4, corresponding experiments and comparisons are provided in section 5. We provide some discussions and analyses in section 6.

2. Related work

All the attacks can be divided into two categories. Some methods can be directly deployed in a black-box attack since they don't require gradients. For example, Chen *et al.* [2] used symmetric difference gradient to estimate the gradient and Hessian. Su *et al.* [23] utilized differential evolution to find the optimal solution. Zhao *et al.* [27] built a generator to map the latent vector to the adversarial examples, and used search algorithms to search the effective noise. However, all these methods have to compromise on adversarial goals or perturbation scope. [2] has to optimize on every single image. [23] aimed to generate adversarial examples by only modifying one pixel and only experimented on small images. [27] is non-targeted attack.

Most other methods have to get access to the victim model, but due to the transferability of adversarial examples proposed by Papernot *et al.*[20], they are able to be transferred to other victim models [22], [6], [21], [16], [1] or even the black-box services [14]. However, it's still hard to ensure good transferability when considering the distortion of adversarial examples, time consumption and targeted attack. [24] first used L-BFGS method to generate the adversarial examples, but it's time-consuming. [6] and its extended methods [22], [11], [3], [25] performed only one step gradient at each pixel to speed up the optimization. [21] computed Jacobian matrix of given sample trying to make most significant changes with smallest perturbations. [16] further reduced the intensity of perturbation by considering the classifier is linearized around the samples. [1] defined a new objective function to describe the distance between sources and adversarial examples for better optimized the distance and penalty term. [14] discovered targeted attacks are harder to transfer than non-targeted attacks and optimized on ensemble deep neural networks to improve transferability. However, all these optimization-based methods are individual attacks, which means they have to optimize on each single source image. [15] first found the universal perturbation over large dataset but it is unable to be deployed to targeted attacks. In this paper, we show the existence of

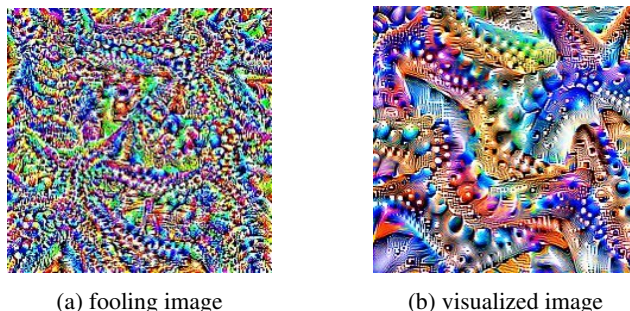


Figure 2: The comparison of fooling image and visualized image of class 'starfish' in VGG19. Both images maximize the activation of the last fully connected layer before softmax.

a universal mapping from the source images to the transferable and targeted adversarial examples with small distortions.

3. Low frequency fooling image

Before going into the adversarial examples, let's discuss about the fooling images. This nomenclature is adopted from [17], which means the images that are meaningless to humans, but the networks classify them to certain classes with high confidences.

For producing a fooling image, we solve the following optimization problem:

$$I_f = \arg \max P(y|I_f) \quad (1)$$

where I_f denotes the fooling image, $P(y|I_f)$ denotes the classifier's confidence of the targeted label y when inputting image I_f . If the neural networks are differentiable with respect to their inputs. We can use derivatives to iteratively tweak the input towards the goal. The way to produce fooling images very like the way to visualize the network [19]. The difference is the target layer and constraint. Neural network visualization optimizes the layers which it aims to visualize. And for recognition, neural network visualization will add extra constraints to this optimization problem, forcing the goal to lie in the low frequency space. A contrast of fooling image and network visualization result is shown in Figure 2. A question is why the networks will naturally produce the high frequency unrecognizable noise. Odena *et al.* [18] indicated they may be closely related to the structure of the networks, especially the strided deconvolutional layers and the pooling operations. Since Odena *et al.* [18] pointed out the deconvolution operations are the root of the grid effect, one possible interpretation is when we leverage the gradients going backward from the targeted label, as what we do when solving Eqn. (1), every convolution layer in the network will serve as a deconvolutional layer.

Therefore, the gradients will have to go through excess deconvolutional layers (generally 2 or 3 deconvolutional layers are able to produce grid effect). The grid effect is sequentially magnified by these deconvolutional layers, and finally become these high frequency noises.

If these high frequency noises are closely related to the structure of the networks, are the low frequency fooling images can be unrelated to the structure of networks, thus being more general and transferable than these high frequency ones? To answer this question, we tried several methods to constrain the high frequency noises in the fooling images.

1. Transformation Robustness (TR) constrains high frequencies by applying small transformations to the fooling images before optimization. Here, we rotate, scale and jitter the images. The constrained optimization process can be expressed as:

$$I_f^{tr} = \arg \max P(y|T(I_f^{tr})) \quad (2)$$

where T denotes the composition of the specific transformations.

2. Decorrelation (DR) decorrelated the relationship between the neighbour pixels. Here, we do it by using gradient descent in the Fourier basis, as what [19] did to visualize the network. It can be expressed as:

$$\begin{aligned} \theta &= \arg \max P(y|\mathcal{F}(\theta)) \\ I_f^{dr} &= \mathcal{F}(\theta) \end{aligned} \quad (3)$$

where \mathcal{F} denotes Fourier transform.

3. Transformation Robustness and Decorrelation (TR and DR) are able to combine together to generate fooling images, which is expressed as:

$$\begin{aligned} \theta &= \arg \max P(y|T(\mathcal{F}(\theta))) \\ I_f^{tr\&dr} &= \mathcal{F}(\theta) \end{aligned} \quad (4)$$

4. Gradient optimized Compositional Pattern Producing Network (Gradient-CPPN) uses CPPN to map the source images to the adversarial examples. CPPN is a neural network that map a position of the image to it's color. Thus, the frequency of the outputted fooling image is related to the architecture of CPPN. The simpler the structure of the network, the lower the frequency of getting images. This method optimizes CPPN parameters by the gradients of the victim model, which can be expressed as:

$$\begin{aligned} CPPN(M_p) &= \arg \max P(y|CPPN(M_p)) \\ I_f^{gcppn} &= CPPN(M_p) \end{aligned} \quad (5)$$

where M_p is a 2-D position map.

5. CPPN encoded Evolutionary Algorithms (EA-CPPN) is proposed by [17]. This method uses CPPN encoded image to represent genomes and uses EA to optimize.

We choose VGG16 as our victim model to train the fooling images and test the results on Clarifai.com, which is a black-box image classification service. We shown some examples in Figure 3. We find that consistent with our hypothesis, low-frequency images can fool Clarifai.com into classifying them as targeted or related classes, while high-frequency noises are fail to fool the system. In all these low-frequency images, gradient optimized CPPN performs better than the other methods. As our goal is to generate the transferable targeted adversarial examples, these low-frequency fooling images are not enough. In the next section, we will introduce how we leverage these low-frequency images to generate transferable targeted adversarial examples. For the convenience, in the following, we refer to these constrained low-frequency fooling images as I_{lf} , and unconstrained high-frequency fooling image as I_{hf} .

4. Generating adversarial examples

4.1. Method

For generating the adversarial examples, we aim at mapping the distribution of the source images to the targeted adversarial distribution. The samples in this distribution should maintain the similarity with the source images in the low level (pixel level), but have the similar high-level features with fooling images. These high-level features preserve the attribution of the fooling images to ensure the success of the attack and also, we assume, the low-frequency property to ensure the transferability. We prove this assumption by comparing the high-level features of fooling images with different frequencies. We find the mean and variance of different distributions cluster together, which denotes the I_{lf} have some specific properties to ensure their transferabilities.

We build a conditional image generation function to shift the original source image distribution to inherit I_{lf} distributions' properties. Put formally, let I_s and I_f be the source images and fooling images that sampled from two observed distributions $q(I_s)$ and $q(I_f)$, and I_a be the targeted adversarial examples. Our goal is to learn the conditional distribution $q(I_{s-f}|I_f)$ to satisfy:

$$I_a = \arg \max_{I_a \sim q(I_{s-f}|I_f)} P(y|I_a) \quad (6)$$

where I_{s-f} denotes the sample produced by endowing I_s with the properties of I_f .

We build an an encoder-decoder convolutional neural network to serve as the conditional distribution generator. We call it Fooling Transfer Net (FTN). The details of FTN is described in the next section.

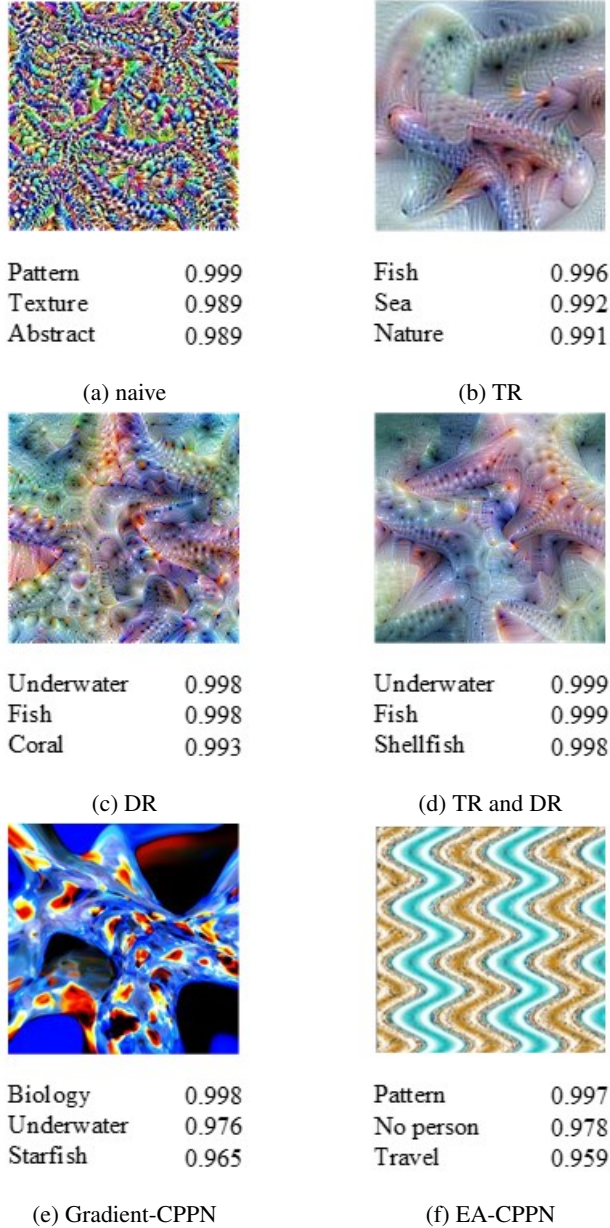


Figure 3: Some samples of high-frequency fooling image: 3a and low-frequency fooling images generated by different methods: 3b-3f. The classes following the images are predicted by Clarifai.com.

4.2. Network structure

Inspired by the image-to-image translation [12], [13] and style transfer task [5]. FTN is built with an encoder E and an AdaIN decoder D . We learn the properties of distribution $q(I_f)$ from its' high-level representations in the victim model, which are denoted as $\phi_i(\hat{I}_f)$, where $\hat{I}_f \sim q(I_f)$ and i denotes the targeted layer of the victim model.

The encoder E consists a sequence of convolutional layers and several residual blocks to encode the source images to a latent vector. The AdaIN decoder is made of two layers AdaIN Residual Blocks followed by several deconvolutional layers. AdaIN Residual Blocks are the residual blocks with adaptive instance normalization layers, will first normalize the activations of a sample in each channel to have a zero mean and unit variance and then scale it with learned scalars and biases. In our translation network, the scalars and biases are got from the means and variances of $\phi_i(\hat{I}_f)$.

Specifically, we extract the $\phi_i(\hat{I}_f)$ in a pretrained classifier, and put them through several fully connected layers to get a certain number of (depending on the number of encoded features) scalars and biases. These scalars and biases are then applied to do the affine transformation to the scaled latent code. Here, we aims at extracting the latent content representations from the source images using the encoder and extracting the class-specific representation from fooling image. Then we shift the latent content code using class-specific representation. In this way, we hope to remain the content information of the original images but adjust them to the targeted attribution.

We supervise the network by the original source images I_s and the fooling images high-level representation $\phi_i(\hat{I}_f)$. I_s constrain the output to maintain maximum content information and $\phi_i(\hat{I}_f)$ constrain the output to have the similar high-level representations with the fooling images. An illustration of FTN is shown in Figure 4.

4.3. Loss function

We constrain the network by three loss function, the content loss L_c , the representation loss L_{rep} , and total variance loss L_{tv} .

The content loss is used to keep content similarity between the adversarial examples and the source images. We use the structural similarity (SSIM) index as our content loss function. SSIM is method to predict the perceived quality of the images. In our contrast experiment, it performs better than traditional L_2 loss function.

The representation loss constraint the output adversarial examples to have similar high-level representations with fooling images in the pretrained classifier. In this paper, we choose VGG19 as our classifier and empirically, choose layer $relu5_2$, $relu5_3$ and $relu5_4$ as the targeted representation. The representation is expressed as:

$$\mathcal{L}_{rep} = \frac{1}{C_j H_j W_j} \|\phi_j(I_a) - \phi_j(I_f)\|_2^2 \quad (7)$$

The total variance loss applies a total variation regularization to punish the reconstruction noise.

The total loss of the network is expressed as:

$$\mathcal{L}_{total} = \mathcal{L}_{SSIM} + \gamma \mathcal{L}_{rep} + \lambda \mathcal{L}_{tv} \quad (8)$$

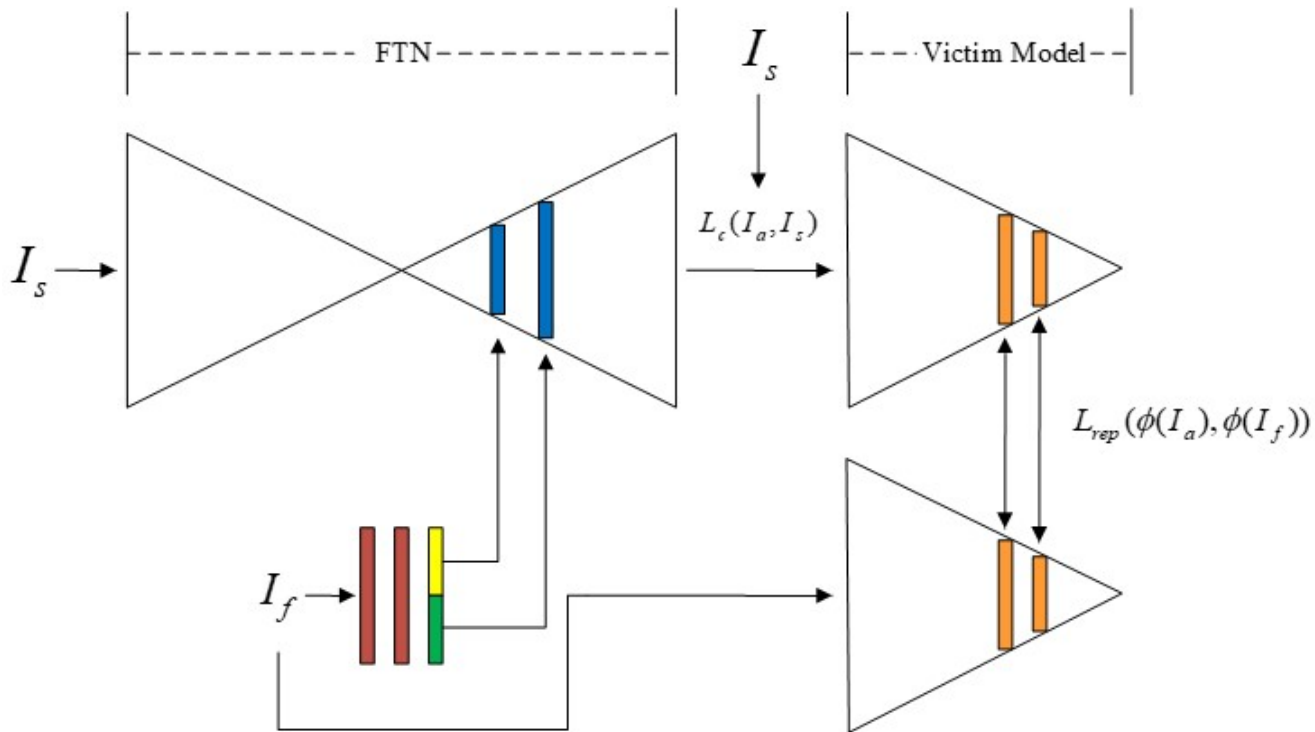


Figure 4: An illustration of FTN, the blue layers denote AdaIN Residual Blocks, the orange layers denote convolutional layers, the brown layers denote fully-connected layers.

where γ and λ are the weight constants of \mathcal{L}_{rep} and \mathcal{L}_{tv} .

5. Experiment

Models: In the paper, we choose a classic classification model: VGG19 as our *training victim model* and test the transferability on the other more delicate classification models, like Inception-v3, ResNet-18, ResNet-50 and Densenet. We denote them as *validation victim models*. There have two points we need to clarify. Firstly, we haven't put a lot of energy on the selection of *training victim model*. That's because relevant experiments have been done by many previous works [6], [14], [8]. And the conclusion has seemed to be uncontroversial: the adversarial examples trained on the more basic models are equipped with more transferability. We don't think our method can be an exception of it. Thus, doing this comparison will be time-consuming, not so meaningful and also distract the readers. Secondly, previous works have shown that using ensemble-based approach can get higher attack success rate [14], [25]. But we only trained our net on a single victim model. That's because we also think our method has no reason to be an exception. Training on a single victim model can preserve more test models to prove the transferability. We welcome the reports that showing our method will be an exception of the previous conclusion.

Dataset: FTN is trained on ILSVRC 2012 classification training set and tested on its' validation set. **Target:** We choose attribution 'starfish' as our default targeted class. We choose this class cause it is almost impossible to tangle with other classes. The features of starfish are distinct from most other objects. Thus it can avoid the circumstance that the model naturally misclassify the source images to the targeted class and then overestimate the performance of our proposed method. The targeted attack of the other classes can be checked in the appendix.

Measure: We measure our results by two important factors: transferability and distortion. The transferability is measured by the *transfer success rate*, which means the percentage of the generated adversarial examples are correctly classified to the targeted label by *validation victim models*. The distortion describes the difference between the generated adversarial examples and the source images. We measured the distortion by *root mean square deviation* (RMSD), which is computed as: $d = \sqrt{\frac{1}{n} \|I_a - I_s\|_2^2}$. We also use the ratio of transfer success rate and distortion, which is denoted as RTD as a measure to compare different methods. Put formally, it is calculated as:

$$RTD = \frac{\text{transfer success rate}}{RMSD} * 100 \quad (9)$$

	Inception-v3	Resnet-18	Resnet-50	Densenet	Clarifai.com
Niave	1%	2%	1%	1%	0%
TR	67%	79%	74%	76%	51%
DR	72%	76%	83%	75%	62%
TR&DR	78%	81%	78%	83%	67%
Gradient-CPPN	96%	94%	91%	93%	86%
EA-CPPN	0%	1%	0%	0%	0%

Table 1: Comparison of fooling images

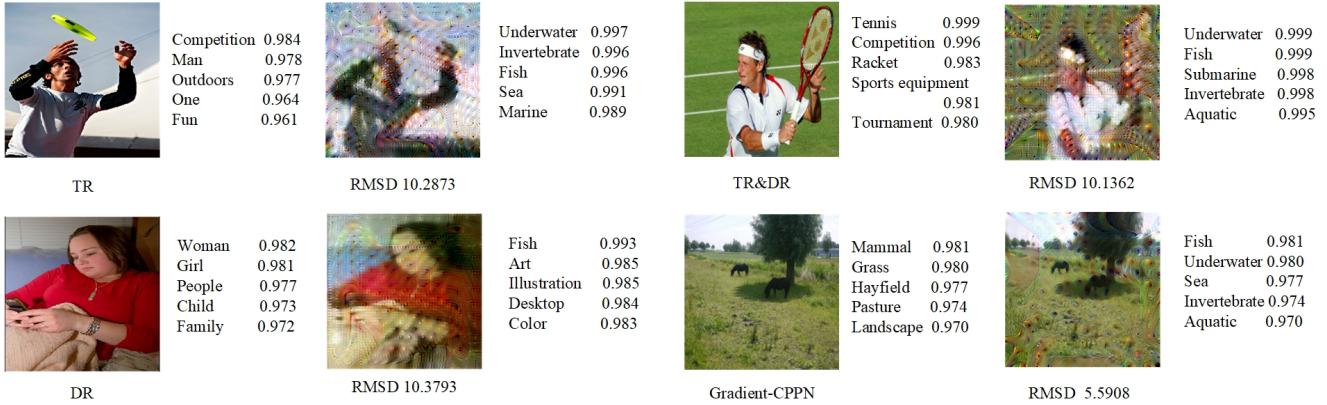


Figure 5: The adversarial examples generated by FTN with different fooling images

5.1. Low-frequency fooling image

In the paper, we proposed low-frequency fooling images and FTN to transfer the source images with them. In this section, we aim to prove I_{lf} are more transferable than I_{hf} and FTN can maintain this transferability.

We have given the examples that I_{lf} are more transferable than I_{hf} above. Here, we do the comprehensive experiment to prove this result. We compare the five high-frequency-constrained methods: CPPN Gradient, CPPN EA, DR, TR, DR+TR and the direct gradient ascent method with no constrain for high-frequency gradients. All the results are trained on *training victim model* and tested on *validation victim models*. The *transfer success rate* of randomly selected 100 samples are shown in Table 1. We can see high-frequency constrained methods generally perform better than direct gradient ascent method, and CPPN Gradient method is the best in them.

And then, we will show FTN can maintain the transferability of I_{lf} . In other words, using more transferable fooling images in FTN can generate more transferable adversarial examples than the others. For the sake of fairness, we adjust the hyper-parameters for every methods to get their best effects. The ratio of *transfer success rate* and distortion is shown in Table 2 and the visual comparison is shown in Figure 5. We can see the better class images can contribute to generate more transferable or less distorted adversarial

examples for the same model.

5.2. FTN

AdaIN normalization We design the AdaIN Residual Blocks in FTN for shifting the latent source distribution by the property of latent class distribution. But in ablation experiment, we see the results are not substantially different. In contrast, the chooses of targeted representation layers and the loss functions play more decisive roles. However, we find the AdaIN residual really help the training process to converge more quickly and the setting of hyper-parameters more easily. The AdaIN Residual Blocks allow more flexibility of the decisive hyper-parameter γ , which denotes the weight of representation loss relative to content loss.

Selection of representations We’ve tried many feasible combination of the targeted representation layers in VGG19. In style transfer, the style representations are generally chose as the activations from low to high. But for generating adversarial examples, the lower representations will endow more superficial similarity between the adversarial examples and fooling images instead of the semantic features. We choose some typical selections and show them in Figure 6.

Loss function For the content loss, we tried L_2 loss function, perceptual loss [10] and SSIM loss. We show the visual comparison in figure[.]. The SSIM loss generates the best visual effect in them. For the representation loss, we

	RMSD	Inception-v3	Resnet-18	Resnet-50	Densenet	Clarifai.com
TR	10.13	3.94	4.34	4.65	4.21	3.00
DR	10.28	4.52	5.33	5.43	5.10	3.94
TR&DR	10.34	6.34	6.81	6.49	7.02	5.41
Gradient-CPPN	5.21	13.32	13.39	12.13	12.23	12.11

Table 2: FTN transferability comparisons using different fooling images



Figure 6: FTN supervised by different layers in VGG19. Content layer denotes the layer of source images in VGG19, style layer denotes the layer of fooling images in VGG19.

tried many loss functions that might be better than simple L_2 loss (e.g. cosine similarity, KL divergence, a bunch of discriminative nets). But unfortunately, none of them works better than L_2 . Intuitively, we think there exists a better loss function for the representations. We hope further researches can find a better way than us.

5.3. Comparison with other methods

Different with most adversarial-examples-generating methods, we learn the universal mapping in the paper instead of doing optimization for every single image. For fairly comparison, we degrade our method to the single image when comparing with the methods that process one particular image every time. These methods include, FG, FGS, Deepfool, JSMA and C&W attack. We do the optimization on VGG19 model and test on *validation victim models* and Clarifai.com. Clarifai.com is a black-box image classification system, no one can get access to its' dataset, network structure and parameters, which is good to test the transferability of adversarial examples. As shown in Table 3, our method can access higher transfer success rate than the other methods for the targeted attack.

We also compare our method with another universal attack [15]. The quantitative results are shown in Table 4.

6. Discussion

In this paper, we proposed low-frequency adversarial examples and proved it is more transferable than the high-frequency ones. However, what low-frequency attacks

mean? Why they can be more transferable than the high-frequency ones? In this section, we attempt to discuss and answer these questions.

Firstly, we find low-frequency attacks and high-frequency attacks are highly different. This difference not only lay on the pixel image but also lay on the classifier representations, which are decisive to the classification (although they will be classified to the same class). This conclusion actually can be confirmed by the observation of difference between I_{lf} generated adversarial examples and I_{hf} generated ones, as shown in Figure[. Cause the generating processes are all the same except the change of class images. But we still do the more rigorous experiments to observe the difference between these representations. We compare the representations of two kinds of fooling images in VGG19 model. Our targeted representations are $relu5_2$, $relu5_3$, $relu5_4$, which we find most effective to supervise our model and most decisive to the final classification. We compute the mean and variance of them and find the mean and variance of the same kind of fooling image are highly similar. This proves although they will be classified to the same class, their high-dimensional features are different.

But what this difference means and how this difference cause the stronger transferability? For answering this question, we analysis the low-frequency attacks and high-frequency attacks on the manifold. In this way, we can think the classification models learn the classified boundaries in a high-dimensional space. The traditional strategy[] is learning a high-dimensional vector and add it to a source image point. These methods constraint the vector can help

	RMSD	Inception-v3	Resnet-18	Resnet-50	Densenet	Clarifai.com
FG	3.56	1%	2%	1%	1%	0%
JSMA	3.21	2%	2%	0%	1%	0%
DeepFool	3.98	28%	33%	34%	31%	1%
C&W	4.55	2%	3%	2%	2%	0%
FTN	3.41	98%	94%	93%	95%	94%

Table 3: Comparison of FTN with different adversarial example generating methods

	RMSD	Inception-v3	Resnet-18	Resnet-50	Densenet	Clarifai.com
Universal	16.25	63%	56%	41%	51%	12%
FTN	5.68	92%	88%	87%	91%	86%

Table 4: Comparison of universal attacks

the source image to escape from its original boundary (non-targeted attack) or pass through another specific boundary (targeted attack). We call the vector perturbation. Since these learning methods attempt to find the smallest vector to make the attack successful, these vectors are highly related to the victim model’s classification boundary. Moosavi *et al.* [15] took them as the normal vectors from the source image point to the boundary. However, although the classification boundary learned by the different models shared some similarities (which make some high-frequency adversarial examples are transferable to some extent), the curvature of the different boundaries can’t be the same. That causes some high-frequency adversarial examples fail to transfer or have to magnify the perturbation to transfer.

Our method decouples the perturbation from the curvature of the boundary surface. Note learning a high-frequency fooling image is finding a point that is classified to the targeted class but which may be sensitive to the difference of the different classification models’ boundaries. And learning a low-frequency fooling image is finding a point that is still classified to the targeted class but less sensitive to the different models’ boundaries. We speculate that is because the low-frequency fooling images are closer to the nature image manifold. And the classification boundaries are trained to be more robust to the nature images than the meaningless noise, since the training datasets are consisted of the nature images. After getting I_{lf} , we then find the point that is near the source image in the pixel space and is close to I_{lf} in the representation space. This constraint condition is independent of the curvature of the boundaries, thus is expected to be more transferable than the previous methods.

7. References

References

- [1] N. Carlini and D. Wagner. Towards evaluating the robustness of neural networks. In *2017 IEEE Symposium on Security and Privacy (SP)*, pages 39–57. IEEE, 2017.
- [2] P.-Y. Chen, H. Zhang, Y. Sharma, J. Yi, and C.-J. Hsieh. Zoo: Zeroth order optimization based black-box attacks to deep neural networks without training substitute models. In *Proceedings of the 10th ACM Workshop on Artificial Intelligence and Security*, pages 15–26. ACM, 2017.
- [3] Y. Dong, F. Liao, T. Pang, H. Su, J. Zhu, X. Hu, and J. Li. Boosting adversarial attacks with momentum. In *Proceedings of the IEEE conference on computer vision and pattern recognition*, pages 9185–9193, 2018.
- [4] V. Fischer, M. C. Kumar, J. H. Metzen, and T. Brox. Adversarial examples for semantic image segmentation. *arXiv preprint arXiv:1703.01101*, 2017.
- [5] L. A. Gatys, A. S. Ecker, and M. Bethge. Image style transfer using convolutional neural networks. In *Proceedings of the IEEE conference on computer vision and pattern recognition*, pages 2414–2423, 2016.
- [6] I. J. Goodfellow, J. Shlens, and C. Szegedy. Explaining and harnessing adversarial examples. *arXiv preprint arXiv:1412.6572*, 2014.
- [7] S. Huang, N. Papernot, I. Goodfellow, Y. Duan, and P. Abbeel. Adversarial attacks on neural network policies. *arXiv preprint arXiv:1702.02284*, 2017.
- [8] A. Ilyas, S. Santurkar, D. Tsipras, L. Engstrom, B. Tran, and A. Madry. Adversarial examples are not bugs, they are features. *arXiv preprint arXiv:1905.02175*, 2019.
- [9] R. Jia and P. Liang. Adversarial examples for evaluating reading comprehension systems. *arXiv preprint arXiv:1707.07328*, 2017.
- [10] J. Johnson, A. Alahi, and L. Fei-Fei. Perceptual losses for real-time style transfer and super-resolution. In *European conference on computer vision*, pages 694–711. Springer, 2016.

- [11] A. Kurakin, I. Goodfellow, and S. Bengio. Adversarial machine learning at scale. *arXiv preprint arXiv:1611.01236*, 2016.
- [12] M.-Y. Liu, T. Breuel, and J. Kautz. Unsupervised image-to-image translation networks. In I. Guyon, U. V. Luxburg, S. Bengio, H. Wallach, R. Fergus, S. Vishwanathan, and R. Garnett, editors, *Advances in Neural Information Processing Systems 30*, pages 700–708. Curran Associates, Inc., 2017.
- [13] M.-Y. Liu, X. Huang, A. Mallya, T. Karras, T. Aila, J. Lehtinen, and J. Kautz. Few-shot unsupervised image-to-image translation. *arXiv preprint arXiv:1905.01723*, 2019.
- [14] Y. Liu, X. Chen, C. Liu, and D. Song. Delving into transferable adversarial examples and black-box attacks. *arXiv preprint arXiv:1611.02770*, 2016.
- [15] S.-M. Moosavi-Dezfooli, A. Fawzi, O. Fawzi, and P. Frossard. Universal adversarial perturbations. In *Proceedings of the IEEE conference on computer vision and pattern recognition*, pages 1765–1773, 2017.
- [16] S.-M. Moosavi-Dezfooli, A. Fawzi, and P. Frossard. Deepfool: a simple and accurate method to fool deep neural networks. In *Proceedings of the IEEE conference on computer vision and pattern recognition*, pages 2574–2582, 2016.
- [17] A. Nguyen, J. Yosinski, and J. Clune. Deep neural networks are easily fooled: High confidence predictions for unrecognizable images. In *Proceedings of the IEEE conference on computer vision and pattern recognition*, pages 427–436, 2015.
- [18] A. Odena, V. Dumoulin, and C. Olah. Deconvolution and checkerboard artifacts. *Distill*, 2016.
- [19] C. Olah, A. Mordvintsev, and L. Schubert. Feature visualization. *Distill*, 2017. <https://distill.pub/2017/feature-visualization>.
- [20] N. Papernot, P. McDaniel, and I. Goodfellow. Transferability in machine learning: from phenomena to black-box attacks using adversarial samples. *arXiv preprint arXiv:1605.07277*, 2016.
- [21] N. Papernot, P. McDaniel, S. Jha, M. Fredrikson, Z. B. Celik, and A. Swami. The limitations of deep learning in adversarial settings. In *2016 IEEE European Symposium on Security and Privacy (EuroS&P)*, pages 372–387. IEEE, 2016.
- [22] A. Rozsa, E. M. Rudd, and T. E. Boulton. Adversarial diversity and hard positive generation. In *Proceedings of the IEEE Conference on Computer Vision and Pattern Recognition Workshops*, pages 25–32, 2016.
- [23] J. Su, D. V. Vargas, and K. Sakurai. One pixel attack for fooling deep neural networks. *IEEE Transactions on Evolutionary Computation*, 2019.
- [24] C. Szegedy, W. Zaremba, I. Sutskever, J. Bruna, D. Erhan, I. Goodfellow, and R. Fergus. Intriguing properties of neural networks. *arXiv preprint arXiv:1312.6199*, 2013.
- [25] F. Tramèr, A. Kurakin, N. Papernot, I. Goodfellow, D. Boneh, and P. McDaniel. Ensemble adversarial training: Attacks and defenses. *arXiv preprint arXiv:1705.07204*, 2017.
- [26] C. Xie, J. Wang, Z. Zhang, Y. Zhou, L. Xie, and A. Yuille. Adversarial examples for semantic segmentation and object detection. In *Proceedings of the IEEE International Conference on Computer Vision*, pages 1369–1378, 2017.
- [27] Z. Zhao, D. Dua, and S. Singh. Generating natural adversarial examples. *arXiv preprint arXiv:1710.11342*, 2017.